

Origin of the Dual Structural Transformation of Trehalose Dihydrate upon Dehydration

J. F. Willart,^{*,†} F. Danede,[†] A. De Gusseme,[†] M. Descamps,[†] and C. Neves[‡]

Laboratoire de Dynamique et Structure des Matériaux Moléculaires, UMR CNRS 8024 - ERT 1018, Université de Lille 1, Bât. P5, 59655 Villeneuve d'Ascq, France, and Laboratoire de Physique Appliquée, Département des Sciences Pharmaceutiques, Centre de Recherches Aventis, 94400 Vitry-sur-Seine, France

Received: March 17, 2003; In Final Form: June 26, 2003

Upon dehydration, trehalose dihydrate transforms either toward a glassy amorphous state or toward a polymorphic crystalline phase depending on the dehydration protocol. Although this duality is now admitted, its origin remains an open question. We present here calorimetric and thermogravimetric experiments clearly showing that the main pertinent physical parameter governing this duality is the instantaneous rate of water release and not the thermal treatment used to dehydrate the sample. The latter, by acting on the rate of water loss, has only an indirect influence on the structure of the dehydrated product. A threshold rate of water removal, above which dehydration produces an amorphous state and below which it produces a polymorphic phase, is also defined.

1. Introduction

The dehydration of crystalline hydrates represents an important group of solid-state transformations that has already been the subject of intensive literature discussion.¹ During dehydration, the crystalline lattice is generally destabilized by the removal of the water molecules and the breaking of the hydrogen bonds that they most often develop with the other molecules. Various kinds of structural transformations can result from this destabilization. One can observe for instance a transformation toward the stable crystalline phase of the anhydrous compound or the formation of a polymorphic metastable phase.² If the dehydration is performed below the glass transition of the corresponding liquid a glassy amorphous state can also be reached.^{2,3} Moreover, the possibility that these direct crystal to glass transformations lead to polyamorphic states similar to those suspected in triphenyl phosphite,^{4,5} in selenium,⁶ and in ice⁷ remains an open question.

The many studies devoted to the dehydration of crystalline hydrates have revealed that the microscopic mechanisms that drive the transformation toward the anhydrous state are often complex and strongly different from one compound to the other one. Up to now, most of the attempts to rationalize these transformations have consisted in drawing criteria capable of classifying the solid-state dehydration processes (see ref 1 for a review). These criteria mainly concern the microscopic mechanisms of water removal and the structural relation between the reactant and the solid-state product.⁸ Though many detailed studies concerning numerous hydrates have already been devoted to this classification aim, any unifying concept able to describe the whole pattern of transformations induced by dehydration could not be established yet. The research of unifying concepts is expected to be enlightened by the study of materials that undergo different kinds of transformations for different dehydration conditions.

Such an unusual behavior is encountered in trehalose (α -D-glucopyranosil, α -D-glucopyranoside), which shows a rich

pattern of nonequilibrium behavior upon dehydration of its dihydrate form (T_{2H_2O}).^{9–12} In particular, recent investigations have clearly revealed a duality between an amorphization process and a polymorphic transformation in the course of the water removal stage.¹² This duality has been found to be very sensitive to the thermal treatment used to dehydrate the sample. A fast dehydration of T_{2H_2O} , induced by a 50 °C/min heating process, has been found to produce amorphous anhydrous trehalose which has clear glassy properties similar to those of conventional glass forming liquids. On the other hand, a slow dehydration, induced by a 1 °C/min heating process, has been found to produce a polymorphic phase α of anhydrous trehalose. For intermediate dehydration rates, a mixed state made of glassy amorphous phase and polymorphic phase α is formed in proportion fixed by the heating rate. A careful reexamination of the abundant literature concerning this sugar also reveals that the structure and the nature of the dehydrated product strongly depend on both the sample characteristics^{13–15} (grain size distribution, crystal defects, ...) and the sample environment^{16–19} (atmosphere, vacuum, encapsulation, ...). These dependences are clearly related to the degrees of easiness with which the water molecules escape from the sample. For instance, at a given temperature, small grains with a lot of cracks obviously dehydrate more rapidly than a big perfect single crystal.

The main goal of this paper is to determine the physical parameters that govern effectively the duality amorphous phase/polymorphic phase during the dehydration of T_{2H_2O} . In a first part, a systematic study of dehydration kinetics induced by different thermal treatments will put forward two possible parameters. They are the rate of water loss itself, and the temperature at which the water molecules are removed. In a second part, we present an original method of analysis by which it will be possible to decide which one of these two parameters mainly governs the duality. This study could be done by the careful control of suitable dehydration protocols in the course of differential scanning calorimetry (DSC) and thermo-gravimetric analysis (TGA) experiments.

* Corresponding author. E-mail: jean-francois.willart@univ-lille1.fr. Tel: 33 (0)3 20 43 68 34.

[†] Université de Lille 1.

[‡] Département des Sciences Pharmaceutiques, Aventis.

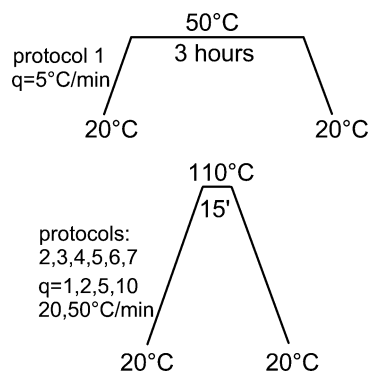


Figure 1. Schematic representation of the seven heating protocols used to dehydrate the samples.

2. Experimental Section

Crystalline α - α trehalose dihydrate was purchased from Fluka. It was more than 99% pure and was used without further purification.

The DSC experiments were performed with the DSC 2920 microcalorimeter of TA Instruments. During all the measurements the sample was placed in an open cell (container with no cover) and was flushed with highly pure helium gas. Temperature and enthalpy readings were calibrated using pure indium at the same scan rates used in the experiments.

The TGA experiments were performed with the TGA 7 of Perkin-Elmer. During all the measurements the sample was placed in an open platinum sample pan and flushed with a highly pure helium gas. The temperature reading was calibrated using the Curie points of alumel and nickel, whereas the mass reading was calibrated using balance tare weights provided by Perkin-Elmer.

It must be noted that the main parameter investigated in this paper is the rate of water loss. Special attention has thus been paid to several dehydration conditions which are known to strongly influence the dehydration kinetics of hydrates.^{1,13,15,20} In particular, each DSC and TGA experiment was performed using a dry atmosphere (He), the same sample mass (~ 6 mg), and open cells that do not hinder the water release. In these conditions the dehydration kinetics observed by TGA and DSC for a given thermal treatment have been found to be identical and reproducible. Moreover, the strict achievement of the programmed thermal treatment for the parallel DSC and TGA experiments was carefully checked (in particular for the greatest heating rates: 50 °C/min) by the systematic monitoring of the $T(t)$ curve (measured temperature vs time).

3. Results

Seven samples of T_{2H_2O} have been dehydrated through seven different thermal protocols schematized in Figure 1. The dehydration experiments have been performed in parallel inside a thermogravimetric analyzer (TGA 7) and inside a calorimeter (DSC TA 2920). The thermogravimetric analyzer was used to characterize the kinetics of water loss *during* the dehydration process whereas the calorimeter was used to characterize the structural and thermodynamic state of the sample *after* the dehydration process.

In **protocol 1**, the T_{2H_2O} sample has been heated to 50 °C at the rate of $q = 5$ °C/min, kept at this temperature during 3 h, and then cooled to 20 °C. The evolution of the dehydrated fraction during the isothermal annealing is shown in Figure 2. It indicates that at 50 °C the dehydration is completed after 2 h of annealing. Run 1 in Figure 3 is the heating scan

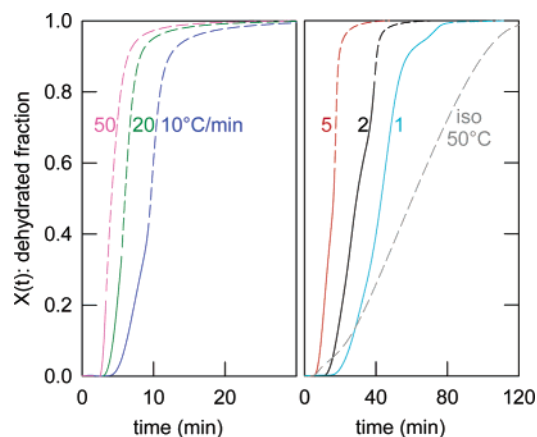


Figure 2. Kinetics of water losses corresponding, from right to left, to the dehydration protocols 1–7 shown in Figure 1. The full part of the curves are related to the water lost during the initial heating ramp, and the dashed part is related to the water lost during the subsequent isotherm (at 50 or 110 °C).

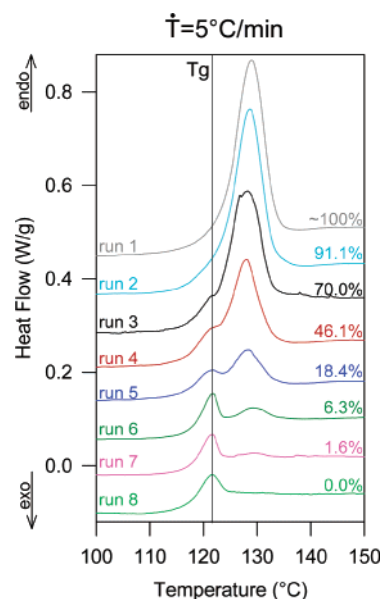


Figure 3. DSC thermograms recorded upon heating at $\dot{T} = 5$ °C/min. Runs 1–7 were respectively recorded after protocols 1–7 of Figure 1 have been completed. Run 8 was recorded after the quench of the melt. The fraction of phase α derived from its melting endotherm is reported on the right-hand side of each thermogram.

($\dot{T} = 5$ °C/min) measured by DSC after the dehydration procedure. It shows clearly a unique endotherm at 125 °C, which has been attributed in a previous paper¹² to the melting of a polymorphic crystalline form (called α) of anhydrous trehalose formed during the dehydration process. By comparison to the heating curve of quenched liquid trehalose (run 8) no sign of the endothermic overshoot ending the C_p jump at T_g could be detected in run 1. This indicates that no amorphous trehalose was produced during the dehydration process. The transformation $T_{2H_2O} \rightarrow \alpha$ thus appears to be total and the enthalpy of melting can be estimated: $\Delta H\alpha = 11.6$ kJ/mol.

In **protocol 7**, the T_{2H_2O} sample has been heated to 110 °C at the rate of $q = 50$ °C/min, kept at this temperature for 15 min, and then cooled to 20 °C. The temporal evolution of the dehydrated fraction during the heating temperature ramp and during the isothermal annealing at 110 °C is shown in Figure 2. It indicates that 20% of the sample is dehydrated during the temperature ramp whereas the remaining 80% is dehydrated

during the isothermal annealing at 110 °C. The overall dehydration process is completed in less than 20 min. Run 7 in Figure 3 is the heating scan ($\dot{T} = 5$ °C/min) measured by DSC after the dehydration procedure. It shows clearly a C_p jump at T_g , fully similar to that of the quenched liquid (run 8) whereas the melting peak at 125 °C has nearly disappeared. This indicates that a rapid dehydration in a high temperature range produces anhydrous trehalose in a nearly fully glassy amorphous state.

Protocols 2–6 are fully similar to protocol 7 except that the heating rates to 110 °C are smaller and respectively equal to 1, 2, 5, 10, and 20 °C/min. The temporal evolutions of the dehydrated fraction during the heating temperature ramps and during the isothermal annealing at 110 °C are shown in Figure 2. In each case the dehydration is found to be total. However, for increasing heating rates q , the part of the sample dehydrated during the isothermal stage at 110 °C increases to the detriment of the part dehydrated during the heating stage. Compared to protocols 1 and 7, the dehydration completion time is intermediate and decreases from 80 to 30 min for increasing q values. Runs 2–6 in Figure 3 are the heating scans ($\dot{T} = 5$ °C/min) measured by DSC after the dehydration procedure. They reveal the decrease of the C_p jump at T_g at the expand of melting endotherm of phase α for decreasing heating rate q to 110 °C. This indicates that intermediate heating rates produce a mixed state made of glassy amorphous trehalose and polymorphic phase α , in proportions driven by the dehydration protocol.

The proportion of phase α formed during each dehydration protocol has been estimated from runs 2–7 by the measurement of the enthalpy of melting of phase α . Because the melting of phase α occurs just above T_g , the usual endotherm ending the C_p jump at T_g merges with the endotherm corresponding to the melting of phase α . It is thus difficult to divide the part of the enthalpy related to the glass transition and that related to the melting of phase α . To overcome this problem and to estimate as best as possible the proportion of phase α , we have looked for the linear combinations of runs 1 and 8 that give the best fits of runs 2–7. Because runs 1 and 8 correspond respectively to the pure phase α and to the pure glassy amorphous trehalose, the coefficients of these linear combinations respectively provide the fraction of phase α and the fraction of amorphous trehalose in the dehydrated sample. The proportions of phase α determined by this method are reported on the right-hand side of Figure 3. They appear to strongly depend on the heating rate, varying from 1.6% for $q = 50$ °C/min to 91.1% for $q = 1$ °C/min.

The main goal of this study is to determine the physically pertinent parameters that govern the duality “amorphization/polymorphic transformation” during the dehydration process. These parameters are expected to be the temperature and/or the rate at which the water molecules are removed. The complexity of the problem comes from the intrinsic and unavoidable coupling between these two parameters because, on one hand the rate of water removal is not constant during an isothermal dehydration and on the other hand this rate is also very dependent on temperature. Our experiments show in particular that in the course of a slow heating process most of the water molecules are thus removed slowly in a rather low temperature range whereas in the course of a fast heating process they are removed much more rapidly in a higher temperature range.

4. Analysis and Discussion

In this section we address the question of the origin of the duality “amorphization/polymorphic transformation” during dehydration of T_{2H_2O} . The point is, in particular, to decide

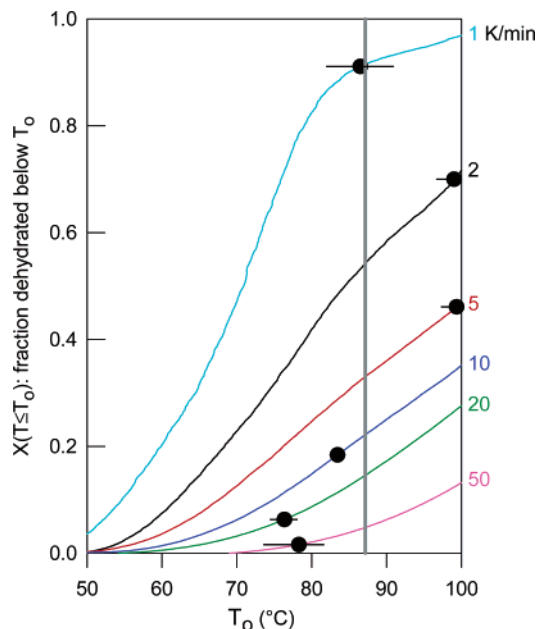


Figure 4. Fraction of the sample $X(T \leq T_0)$ that has been dehydrated below a given temperature T_0 in the course of the dehydration protocols 2–7 (from top to bottom). Data are directly derived from those of Figure 2 using eq 1. The full black circles mark, for each curve, the particular point for which the dehydrated fraction is equal to the fraction of phase α detected in the fully dehydrated sample and reported in Figure 3. In the hypothesis of a threshold temperature T_t these circles are expected to align onto the vertical line which marks their average abscise.

whether this duality is governed by the rate of water loss itself or by the temperature at which this water loss occurs. In other words, we can wonder if there exists a threshold temperature T_t or a threshold rate of water removal R_t above which the dehydration of T_{2H_2O} produces anhydrous amorphous trehalose and below which it produces the polymorphic crystalline phase α .

4.1. Search for a Threshold Dehydration Temperature T_t .

If there exists a threshold temperature T_t , the fraction of the sample dehydrated below this temperature must necessarily be equal to the fraction of the sample transformed to phase α in the course of the overall dehydration process, and this, whatever the thermal treatment used to dehydrate the sample. We have thus determined, for each dehydration protocol, a hypothetical threshold temperature T'_t compatible with the fraction of phase α (X_α) characterizing the fully dehydrated sample. The comparison of these hypothetical threshold temperatures will reveal, a posteriori, if a unique threshold temperature T_t independent of the dehydration protocol can really be defined.

Figure 4 shows the fraction of the sample $X(T \leq T_0)$ that has been dehydrated below a given temperature T_0 in the course of the dehydration protocols 2–7. Data are directly calculated from the kinetics of water loss $X(t)$ shown in Figure 2. These kinetics are made up of N experimental points corresponding to the fractions X_i dehydrated at time t_i when the sample was at temperature T_i : $X(t) \equiv X_i(t_i, T_i)$ for $i = 1$ to N so that

$$X(T \leq T_0) = \sum_{i=1}^N (X_i - X_{i-1}) \sigma_i \quad (1)$$

where

$$\begin{aligned} \sigma_i &= 1 & \text{if} & T_i \leq T_0 \\ \sigma_i &= 0 & \text{if} & T_i > T_0 \end{aligned}$$

This set of curves fully characterizes the thermal pattern of water loss for each dehydration protocol. It shows in particular how the fraction of the sample dehydrated below a given temperature T_0 decreases with increasing heating rate q . For each dehydration protocol, the threshold temperature T'_i has been obtained by determining the temperature T_0 , below which the dehydrated fraction is equal to the fraction X_α of phase α present in the fully dehydrated sample. T'_i is thus the solution of the equation $X(T < T'_i) = X_\alpha$. The points, solutions of this equation, are reported in Figure 4 together with their corresponding error bar. The threshold temperatures T'_i correspond to the abscise of these points.

It appears that the threshold temperatures T'_i spread over a large temperature range and show an apparently erratic variation with the heating rate. They range from 76.3 °C for $q = 20$ °C/min to 99.4 °C for $q = 5$ °C/min leading to a large standard deviation ($\sigma = 9.2$ °C) around their average value ($\langle T'_i \rangle = 87.2$ °C) marked by a dashed line in Figure 4. This strong dispersion associated with the nonoverlapping of the error bars clearly refutes the hypothesis of a unique threshold temperature T_i independent of the dehydration protocol. The duality “amorphization/polymorphic transformation” during the dehydration of T_{2H_2O} is thus clearly not exclusively governed by the temperature at which the water molecules leave the sample.

4.2. Search for a Threshold Rate of Water Removal R_i . During each dehydration protocol, the temporal evolution of the absolute rate of water loss R^{abs} can easily be derived from the experimental dehydration kinetics $X(t) \equiv X_i(t_i, T_i)$ for $i = 1$ to N shown in Figure 2 through the following transformation:

$$R_i^{\text{abs}} = \left(\frac{X_i - X_{i-1}}{t_i - t_{i-1}} \right) (M_o - M_\infty) \frac{1}{\rho_{H_2O}} \quad (2)$$

where ρ_{H_2O} is the water density and $M_o - M_\infty$ is the difference between the mass of the sample before and after the dehydration process. The latter corresponds to the mass of removable water in the initial sample.

Contrary to temperature, the absolute rate of water loss is not an intensive variable. It strongly depends on the mass of sample to be dehydrated. Comparison of the rate of water loss for different samples at different level of dehydration thus requires normalization of the absolute rate of water loss by the mass of the sample not yet dehydrated: $(1 - X_i)M_o$. This normalized rate of water loss (R_i) is thus given by

$$R_i = \frac{1}{1 - X_i} \left(\frac{X_i - X_{i-1}}{t_i - t_{i-1}} \right) \left(\frac{M_o - M_\infty}{M_o \rho_{H_2O}} \right) \quad (3)$$

Because the dehydration has been found to be total for each dehydration protocol, the last term of eq 2 is constant and can be expressed against the molecular weight of anhydrous trehalose ($M_\beta = 342.30$ g mol $^{-1}$) and trehalose dihydrate ($M_{T_{2H_2O}} = 378.33$ g mol $^{-1}$):

$$\frac{M_o - M_\infty}{M_o \rho_{H_2O}} = \frac{1 - (M_\beta/M_{T_{2H_2O}})}{\rho_{H_2O}} = 9.52 \times 10^{-5} \text{ L} \cdot \text{g}^{-1} \quad (4)$$

If there exists a threshold rate of water removal R_i , the fraction of the sample dehydrated with a normalized rate of water removal lower than R_i must necessarily be equal to the fraction of the sample transformed to phase α in the course of the overall dehydration process, and this, whatever the thermal treatment used to dehydrate the sample. The procedure to test this hypothesis is thus exactly the same as that used in section 4.1

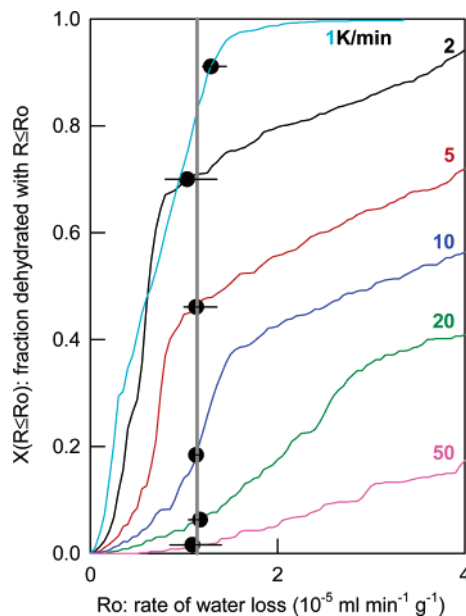


Figure 5. Fraction of the sample $X(R \leq R_0)$ which has been dehydrated with a rate of water loss lower than a given value R_0 in the course of the dehydration protocols 2–7 (from top to bottom). Data are directly derived from those of Figure 2 using eq 5. The full black circles mark, for each curve, the particular point for which the dehydrated fraction is equal to the fraction of phase α detected in the fully dehydrated sample and reported in Figure 3. In the hypothesis of a threshold rate of water removal R_i , these circles are expected to align onto the vertical line which marks their average abscise.

to test the hypothesis of a threshold temperature. We have determined for each dehydration protocol a hypothetical threshold rate of water removal R'_i compatible with the fraction of phase α (X_α) characterizing the fully dehydrated sample. The comparison of these hypothetical threshold rates of water removal will reveal, a posteriori, if a unique threshold rate of water removal R_i independent of the dehydration protocol can really be defined.

Figure 5 shows the fraction of the sample $X(R \leq R_0)$ that has been dehydrated with a rate of water removal smaller than a given value R_0 in the course of the dehydration protocols 2–7. Data are directly calculated from those of Figure 2 as follows:

$$X(R \leq R_0) = \sum_{i=1}^N (X_i - X_{i-1}) \sigma_i \quad (5)$$

where

$$\sigma_i = 1 \quad \text{if} \quad R_i \leq R_0$$

$$\sigma_i = 0 \quad \text{if} \quad R_i > R_0$$

For each dehydration protocol, the hypothetical threshold rate of water removal R'_i has been obtained by solving graphically the equation $X(R \leq R_i) = X_\alpha$. The points solution of this equation are reported in Figure 5, together with their corresponding error bar. The threshold rate of water removal R'_i are given by the abscises of these points.

Contrary to the threshold temperatures T'_i , the threshold rates of water removal R'_i appear to be very weakly dispersed ($\sigma = 0.078 \times 10^{-5}$ mL min $^{-1}$ g $^{-1}$) around their average value marked by a dashed line in Figure 5. This vertical straight line fits perfectly the data of Figure 5 and intersects all the error bars. It is thus possible to define a threshold rate of water removal ($R_i = \langle R'_i \rangle = 1.14 \times 10^{-5}$ mL min $^{-1}$ g $^{-1}$), above which

dehydration of T_{2H_2O} produces amorphous trehalose and below which it produces the polymorph α . The results also show that the dependence of the threshold rate of water removal on temperature, if any, is very weak. This rather unexpected behavior could result from the sub- T_g character of the thermal treatments used to dehydrate the samples. In such a temperature range the molecular mobility of anhydrous trehalose is obviously much weaker than that of the escaping (diffusing) water molecules. The structural modifications induced by sub- T_g dehydrations are thus more related to the more or less energetic departure of the water molecules than to the structural reorganization (or disorganization) of the remaining trehalose molecules themselves.

5. Conclusion

The duality amorphous phase/polymorphic phase that characterizes the dehydration of T_{2H_2O} has been investigated for a variety of dehydration protocols. The results have been obtained by coupling DSC experiments to TGA experiments to characterize in real time the water losses during the dehydration processes. The analysis of the results in terms of instantaneous dehydration rates clearly shows that the duality amorphous phase/polymorphic phase is mainly driven by the rate of water loss, and not by the thermal treatment used to remove the water molecules. The latter, by acting on the rate of water loss, has only an indirect influence on the structure of the dehydrated product. It was also possible to define a threshold rate of water removal (R_t) above which the dehydrated regions become amorphous and below which they transform toward the polymorphic phase α . Such a behavior suggests that the structural evolution of T_{2H_2O} upon dehydration results from an athermal driving mechanism similar to that of mechanical milling or irradiation.^{21,22}

Acknowledgment. This work was performed in the framework of an Interreg II grant between Nord-Pas de Calais and Kent. A.D.G. is grateful to Aventis and Nord Pas de Calais region for their fellowship support.

References and Notes

- (1) Galwey, A. K. *Thermochim. Acta* **2000**, 355, 181.
- (2) Ono, M.; Tozuka, Y.; Oguchi, T.; et al. *Int. J. Pharm.* **2002**, 239, 1.
- (3) Onodera, N.; Suga, H.; Seki, S. *Bull. Chem. Soc. Jpn.* **1968**, 41, 2222.
- (4) Ha, A.; Cohen, I.; Iee, M.; et al. *J. Phys. Chem. Solids* **1996**, 100, 1.
- (5) Hedoux, A.; Guinet, Y.; Descamps, M. *Phys. Rev. B* **1998**, 58, 1.
- (6) Lu, K.; Guo, F. Q.; Zhao, Y. H.; et al. *Nanocryst. Mater.* **1999**, 2–6, 43.
- (7) Mishima, O. *Nature* **1996**, 384, 546.
- (8) Petit, S.; Coquerel, G. *Chem. Mater.* **1996**, 8, 2247.
- (9) Sussich, F.; Urbani, R.; Princivalle, F.; et al. *J. Am. Chem. Soc.* **1998**, 120, 7893.
- (10) Sussich, F.; Princivalle, F.; Cesaro, A. *Carbohydr. Res.* **1999**, 322, 113.
- (11) Macdonald, C.; Johari, G. P. *J. Mol. Struct.* **2000**, 523, 119.
- (12) Willart, J. F.; De Gussemme, A.; Hemon, S.; et al. *J. Phys. Chem. B* **2002**, 106, 3365.
- (13) Taylor, L. S.; York, P. *J. Pharm. Sci.* **1998**, 87, 347.
- (14) Taylor, L. S.; Williams, A. C.; York, P. *Pharm. Res.* **1998**, 15, 1207.
- (15) Taylor, L. S.; York, P. *Int. J. Pharm.* **1998**, 167, 215.
- (16) Reisener, H. J.; Goldschmid, H. R.; Ledingham, G. A.; et al. *Can. J. Biochem.* **1962**, 40, 1248.
- (17) Ding, S. Fan, J.; Green, L.; et al. *J. Therm. Anal.* **1996**, 47, 1391.
- (18) Nagase, H.; Endo, T.; Ueda, H.; et al. *Carbohydr. Res.* **2002**, 337, 167.
- (19) Sussich, F.; Bortoluzzi, S.; Cesaro, A. *Thermochim. Acta* **2002**, 391, 137.
- (20) Agbada, C. O.; York, P. *Int. J. Pharm.* **1994**, 106, 33.
- (21) Martin, G.; Bellon, P. *Solid State Phys.* **1997**, 50, 189.
- (22) Willart, J. F.; De Gussemme, A.; Hemon, S.; et al. *Solid State Commun.* **2001**, 119, 501.